Health Impacts of Lake Desiccation

Lena Harris

1 Introduction

Increased water demand for agricultural and urban use has caused lakes around the world to shrink, a process known as desiccation (Wurtsbaugh et al., 2017). This includes the Great Salt Lake in Utah, which as of January 2025 had shrunk by 30% (1,059km^2) relative to historic levels. In addition to the direct economic and ecologic impacts of lake desiccation, there are also potential health concerns arising from possible increases in air pollution due to wind blown lake bed (playa) dust. While other desiccated lakes are known to contribute to poor air quality (Owen's Lake in California for example is the largest point source of PM_{10} pollution in the US (EPA, 2017)), it is unclear to what extent desiccation of the Great Salt Lake will have similar impacts due to differences in playa soil structure and chemical composition (Attah et al., 2024; Perry, Crosman, and Hoch, 2019).

This paper quantifies the infant health impacts from desiccation of the Great Salt Lake using a causal inference framework. We first use daily pollution data from a network of air quality monitors to quantify the change in local air pollution due to playa dust. This analysis uses temporal variation in lake levels and wind conditions in a difference-in-difference style framework. We then apply the same framework to create predictions of playa dust concentrations at given points over time. These predictions are used to estimate the health impact associated with increased dust exposure due to lake desiccation. We measure health with individual-level birth outcomes, and identify exposure to playa based on the last three months of pregnancy for the primary analysis.

We find desiccation of the Great Salt Lake leads to worse local air quality, with a 100km^2 increase in playa area increasing $PM_{2.5}$ concentrations by about $0.5\mu g/\mathrm{m}^3$. Multiplying the 30% decline in lake area by this effect translates to an extra $5\mu g/\mathrm{m}^3$ of $\mathrm{PM}_{2.5}$.[1] While the largest air pollution increases are primarily concentrated in closer proximity to the lake (30km), there are far reaching, weaker effects up to 100km away from the lake.

The worsened air quality translates into large, though statistically imprecise, reductions in health. A $100\mathrm{km}^2$ increase in playa area is associated with increased incidence of pre-term birth by up to 1%, decreased birth weight by about 1.75g, and a 3 percent reduction in the number of births. Comparing these results to meta-analysis estimates of the effect of $\mathrm{PM}_{2.5}$ on birth outcomes (Stieb et al., 2012), our estimated effects are all relatively large – though still fall within the 95% confidence intervals of the meta-analysis estimates. Our estimated health impacts underscore the need for policy makers to consider health externalities arising from lake desiccation when considering water allocations and diversions.

This paper is the first to quantify the impact of lake desiccation on infant health in nearby communities using a causal framework. Existing work documents associations with adverse health outcomes, with most analyses relying on cross-section comparisons with respect to lake proximity (Farzan et al., 2019; Gomez et al., 1992). While some work uses temporal variation in lake levels (Jones and Fleck, 2020), these analyses are unable to fully account for potential spatial confounding. By exploiting both spatial and temporal variation in lake levels and wind conditions, our analysis is able to flexibly control for confounding more fully. Having a better estimate of the true impact of desiccation on health is important for accurate welfare analyses of alternative water management decisions.

This paper also contributes to the existing literature by modeling heterogeneous, localized pollution changes from desiccation with reduced form econometric tools. While the analysis frameworks we use for modeling playa dust have been commonly used in economics research on air pollution from other sources (Kim and Gillingham, 2025; Schlenker and Walker, 2016; Currie and Walker, 2011; Hill et al., 2024), they have yet to be applied to lake desiccation. Instead, lake desiccation emissions have generally been measured with extremely local dust sample collection methods (Goodman et al., 2019; King et al., 2011) or through computationally intensive particle transport models (Abman, Edwards, and Hernandez-Cortes, 2024). To the best of our knowledge, only Jones and Fleck (2020)

[1] The EPA air quality standard for $\mathrm{PM}_{2.5}$ is 9 $\mu g/\mathrm{m}^3$ as of February 7th, 2024 (EPA, 2024).

predict playa dust using econometric tools, though they abstract from spatial heterogeneity in their analyses. The findings from our paper show that simpler models can capture local variation in pollution arising from desiccation. This is useful for subsequent analyses examining alternative outcomes or other lakes and contexts.

2 Data

2.1 Infant Health

Birth record data containing information on infant health and parental characteristics is pulled from the National Center for Health Statistics National Vital Statistics system. This data is a compilation of federal birth certificates, so it covers the universe of births in the US between 1990 and 2022. Each birth record is geocoded at the pregnant individual's county of residence, and contains information on infant health and parental covariates at the time of birth, which is reported as the birth month and year. From this data, we select our sample for the health analyses by selecting births that occur to individuals residing within 300km of the Great Salt Lake and meet certain criteria: is a live birth, is a singleton birth, has birth weight within reasonable bounds (500-5,000g), and has gestation age within reasonable bounds (22-42 weeks). Our resulting sample consists of 1,369,363 births total, with 244,216 overlapping the time frame of available air pollution data (2016-2022).

2.2 Air Pollution

Measurements of local air pollution concentrations are from PurpleAir. This data consists of histories of measured $PM_{2.5}$, PM_{10}, and PM_1 for community based air pollution monitors.[2] We collect daily average pollution reports for all outdoor monitors within 300km of the Great Salt Lake over the time frame from January 1, 2016 through December 30, 2024. The final sample used in the analyses is an unbalanced panel of 604,005 daily observations over 540 monitors. Descriptive statistics of these monitors are shown in the first column of Table 1.

[2] The measured pollutants are particulate matter (PM), where the subscript reflects the maximum particle diameter in micrometers. PM is measured in micrograms per cubic meter, $\mu g/\mathrm{m}^3$.

Table 1: Descriptive Statistics

	PurpleAir	Centroids
Panel A: Exposure Variables		
Playa area (km^2)	1078.1	1040.6
	(119.4)	(129.5)
Distance to lake (km)	0.0538	0.124
	(0.0595)	(0.0977)
Wind Direction	-0.176	-0.0439
	(0.478)	(0.504)
Wind speed	1.741	1.863
	(0.571)	(0.753)
Panel B: Air Pollution		
PM_{10} ($\mu g/m^3$)	7.816	7.184
	(12.71)	(10.34)
$PM_{2.5}$ ($\mu g/m^3$)	6.514	6.364
	(6.408)	(5.735)
PM_1 ($\mu g/m^3$)	4.337	4.155
	(6.726)	(5.588)
Panel C: Infant Health		
Birth weight		3291.8
		(506.9)
Gestation age		38.56
		(1.837)
Number of points	540	27
Number of pollution observations	604,005	62,603
Number of birth observations		248,200

Notes: Table presents descriptive statistics for the PurpleAir pollution monitor data set and the county population-weighted centroids linked to births. In Panels A and B, each observation is at the point-day level, where a point reflects a pollution monitor or county centroid. For Panel C, each observation is a birth.

The advantages of the PurpleAir data are twofold. First, the pollutant measures reflect true particulate counts at the monitor's location, rather than being modeled estimates derived from satellite data. Second, by using community based monitors the available monitor network is relatively densely populated, as shown in Figure 1. However, because the data is crowd sourced and not subject to data quality reviews, we follow guidelines from the US Environmental Protection Agency (EPA) to identify and remove observations with data quality concerns, as well as apply a correction for overstated levels at high $\text{PM}_{2.5}$ concentrations (Barkjohn, Clements, and Holder, 2022).[3] This process results in about 9% of the raw observations being removed from the sample. Our analyses will focus primarily on $\text{PM}_{2.5}$ since the PurpleAir data aligns more closely with validated EPA monitor data, as shown in Figure A1.

Because the birth data is geocoded at the county level, for our analyses we construct an estimate of air pollution at the county population weighted centroid using the PurpleAir monitors. For each county centroid c on day t, we estimate pollution as the inverse distance weighted average of readings from PurpleAir monitors within 100km of the centroid.

$$\text{PM}_{2.5ct} = \frac{\sum_m \frac{1}{Distance^2_{cm}} PM_{mt}}{\sum_m \frac{1}{Distance^2_{cm}}} \tag{1}$$

We use a scaling parameter of 2, where a larger parameter places more weight on closer observations. This parameter was calibrated by regressing $\text{PM}_{2.5}$ measures from US EPA managed air pollution monitors on an inverse distance weighted average of PurpleAir $\text{PM}_{2.5}$ measures at the EPA monitors' locations and selecting the parameter which maximized the R^2 from that regression.[4]

[3]Each PurpleAir monitor reports two estimates of each pollutant. The EPA guidelines identify data from a monitor as being valid if the two measurements for $\text{PM}_{2.5}$ are either within $5\mu g/\text{m}^3$ or 70% of each other (Barkjohn, Clements, and Holder, 2022). We further treat measurements with particulate measures over $1{,}000\mu g/\text{m}^3$ as missing, and trim the top and bottom 0.5% of the remaining distribution.

[4]The EPA monitor data is from the Air Quality System (AQS) database. The max R^2 value achieved through the calibration process is 0.75. Figure A1 of the Appendix plots of the IDW average $\text{PM}_{2.5}$ estimates and true $\text{PM}_{2.5}$ measures.

Figure 1: Mapping of Data

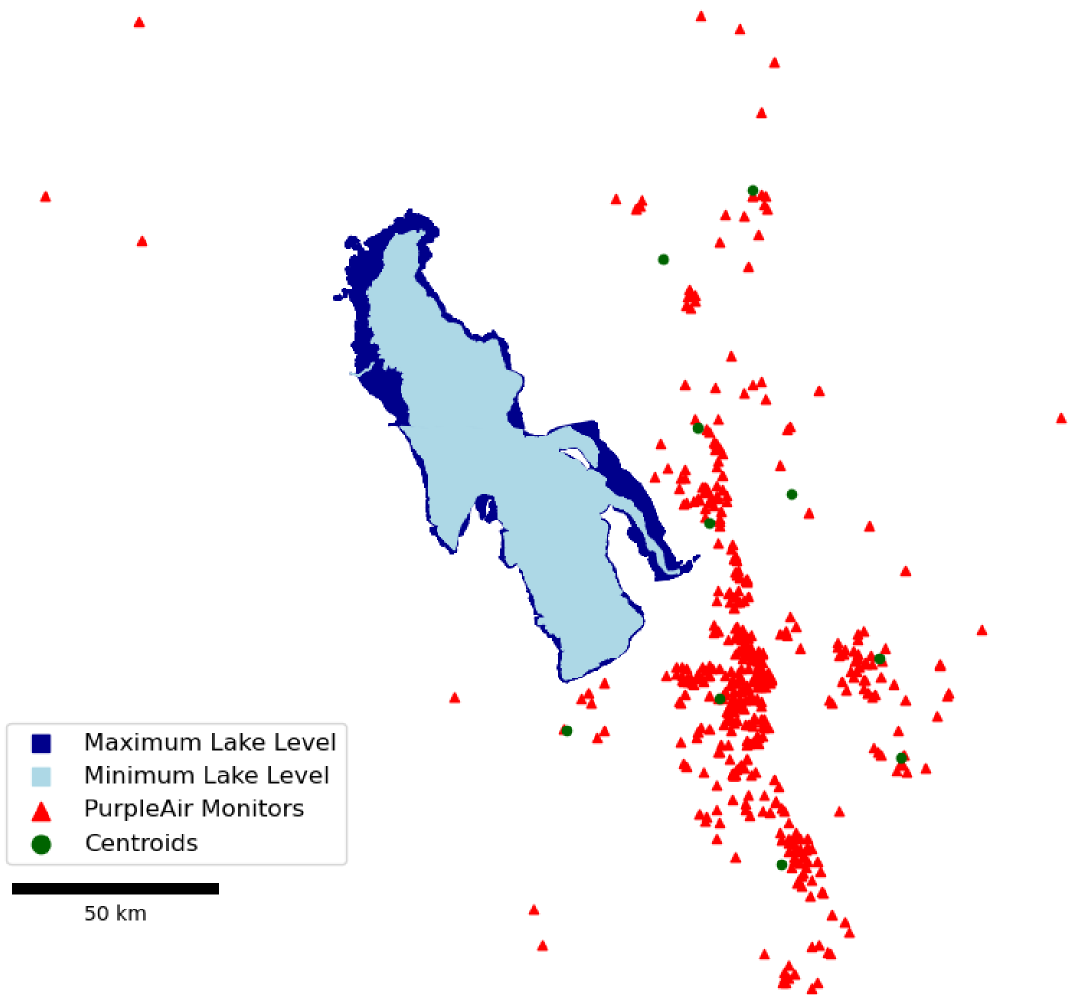

Notes: Map shows the spatial extent of the Great Salt Lake at its largest extent as well as at the lowest levels in the sample. Points denote surrounding PurpleAir pollution monitors and county population weighted centroids that are within 100km of the lake.

Figure 2: Playa Area Over Time

Notes: Figure shows playa area over time between 2000 and 2024 from USGS water level gauges. The vertical dashed line denotes 2016, the start of the PurpleAir pollution sample.

2.3 Playa Exposure

Temporal variation in exposed playa area is calculated from daily readings of water level gauges maintained by the US Geological Survey. We pull the histories of water levels since 1990 for two gauges in the lake, one in the north half and one in the south.[5] These elevation measures are then mapped to total lake surface area following the crosswalks documented in Baskin (2005) and Baskin (2006).[6] Total playa area is then calculated as the difference between lake surface area on a given day t and the maximum possible lake area (3,613 km^2).

$$\text{Playa Area}_t = \text{Maximum Possible Surface Area} - \text{Lake Surface Area}_t \tag{2}$$

The evolution of playa area over time is shown in Figure 2.

Variation in a given location's exposure to playa dust is driven in part by wind conditions, which are captured by wind vectors from Copernicus Climate Change Service.

[5]Construction of a railroad causeway across the lake in 1959 essentially divided the lake into two halves, north and south, with potentially different water levels. We use water level measures for the south half from the gauge USGS 10010000 Great Salt Lake at Saltair Boat Harbor, UT and for the north half from the gauge USGS 10010100 Great Salt Lake near Saline, UT.

[6]Total surface area is constructed by summing the surface area of each lake half.

These data consist of gridded hourly wind vectors since 1990 to present, and are available at a spatial extent of $0.1° \times 0.1°$. Each vector is characterized by a u- and v-component which reflect the speed of air moving towards the east and north, respectively. The magnitude of the wind vector denotes wind speed, while the angle indicates the direction towards which wind is moving, so that a wind going towards the north would have a Cartesian angle of 90° and a wind going towards the east would have a Cartesian angle of 0°.

We operationalize the hourly wind vectors, following Schlenker and Walker (2016), by creating a daily measure of the relative distance between the wind direction and the direction that would result in a point being exactly downwind of the lake centroid. To construct this measure, we use the following process. First, for every point of interest, p, we identify the angle Θ_p between a vector connecting the lake centroid to the point and a (1,0) vector following the x-axis, where the lake centroid is located at the point (0,0). Θ_p is the angle such that wind blowing in that direction will result in point p being exactly downwind of the lake centroid. Second, we map each point to the hourly wind directions from the grid cell overlapping the point and average them to get a daily average wind direction, denoted θ_{pt}. Third, we calculate the distance between the observed wind direction and the downwind angle using the following equation,

$$W_{pt} = cos(\Theta_p - \theta_{p,t}) \tag{3}$$

W_{pt} will be equal to one if the point is perfectly downwind from the lake centroid, equal to negative one if the point is perfectly upwind, and approach zero as the wind becomes perpendicular to the downwind vector.

3 Methodology

This section presents the methodology used to identify the effect of exposure to playa dust on infant health outcomes. To account for measurement issues and bias from spatial sorting, we use a two stage estimation process where our identifying variation in playa dust comes from exogenous variation in wind direction, lake levels, and distance from the lake. The first stage estimation uses two alternative difference-in-difference style frameworks, where the lake level impacts the amount of playa dust and wind direction and distance from the lake change exposure to the dust. The second stage estimation uses the average of the instrumented daily playa exposure over the last three months of pregnancy to estimate the impact of aggregate playa exposure on infant health.

3.1 First Stage: Air Pollution

We first quantify the impact of increased playa on local pollution concentrations using the daily PurpleAir pollution data for PM_{10}, $PM_{2.5}$, and PM_1 and exploiting variation in playa area and weather patterns over time. We initially outline a simplified analysis using a near-far difference-in-difference framework, comparing across space changes in PM due to changes in playa area. This type of analysis is commonly used and provides readily interpretable results, but abstracts from key aspects underlying the true data generating process. To better predict PM for the subsequent health analyses, we introduce a model which interacts the simpler model with local wind conditions following Schlenker and Walker (2016). This second model is more of a black box approach, but provides more spatially disaggregated pollution predictions.

The first model uses a difference-in-difference framework, where the first difference is with respect to playa area and the second is with respect to distance from the lake.

$$\text{PM}_{pt} = \sum_{d \in D} \beta_d \mathbb{1}(\text{Distance}_p \in d) \times \text{Playa Area}_t + E'_{pt}\gamma + \phi_p + \phi_t + e_{pt} \tag{4}$$

The outcome of interest is one of the three PM concentrations (PM_{10}, $PM_{2.5}$, PM_1) at monitor p on day t. The right hand side of the equation includes a set of 11 environment covariates E_{pt} which consists of precipitation, minimum and maximum temperature, minimum vapor pressure deficit, their squares, average wind speed, and relative wind angle (W_{pt} from Eq. 3) interacted with indicators for whether it is upwind or downwind (negative or positive).[7] We also include point and time fixed effects, ϕ_p and ϕ_t respectively. The coefficients of interest

[7] Precipitation, temperature and vapor pressure deficit are from PRISM Spatial Climate datasets and measured on a 4km grid.

are the set of β coefficients, where β_d is the coefficient on the interaction between playa area and an indicator for the distance between the lake and the monitor being in bin d.[8] We define 10 distance bins with cutoffs at 10, 20, 30, 50, 75, 100, 125, 150, 200, 250, and 300 km. In combination, the set of βs trace out the effect gradient of an increase in playa area over space, relative to the omitted distance bin (250-300km).

The second model augments Equation 4 by incorporating variation in local wind conditions which could drive differential transport of playa dust.

$$\begin{aligned}
\text{PM}_{pt} = {} & f(\text{Playa Area}_t, \text{Distance}_p, \text{Wind Speed}_{pt}, \text{Summer}_t, \mathbb{1}(W_{pt} > 0) \times W_{pt}) \\
& + f(\text{Playa Area}_t, \text{Distance}_p^2, \text{Wind Speed}_{pt}, \text{Summer}_t, \mathbb{1}(W_{pt} > 0) \times W_{pt}) \\
& + f(\text{Playa Area}_t, \text{Distance}_p, \text{Wind Speed}_{pt}, \text{Summer}_t, \mathbb{1}(W_{pt} < 0) \times W_{pt}) \\
& + f(\text{Playa Area}_t, \text{Distance}_p^2, \text{Wind Speed}_{pt}, \text{Summer}_t, \mathbb{1}(W_{pt} < 0) \times W_{pt}) \\
& + E_{pt}\gamma + \phi_p + \phi_m(t) + e_{pt} \qquad (5)
\end{aligned}$$

Similar to Equation 4, the outcomes of interest are daily PM measures and the model includes point fixed effects. Unlike before, the time fixed effect has been replaced with a linear year trend and a calendar month fixed effect. Additionally, the impact of playa area is now captured by the functions $f(\cdot)$ which denote the full interactions of the arguments. Notice first that distance from the lake now enters as a quadratic rather than a categorical variable. Second, wind speed is included to capture the potential for higher speed winds to both clear the air while also transporting particles further. Third, an indicator for the observation being between April and September (Summer_t) is included to capture seasonality of wind patterns, an especially important aspect for Salt Lake which is notorious for winter inversions. And notice lastly that the constructed wind direction measure W_{pt} is interacted with indicators for upwind and downwind to allow the effect of the relative angle to vary.

For both models, the marginal effect of playa area plausibly captures changes in PM due uniquely to lake desiccation. As playa levels evolve over time, the temporal controls and point fixed effects capture variation in PM driven by persistent location specific fea-

[8] Distance between the lake and a point is measured from the lake boundary at the maximum lake surface area (3,613 km^2). Shapefiles of the lake boundary are publicly available from the Utah Department of Natural Resources.

tures or area wide temporal variation (such as seasonality or long run pollution reductions). Additionally, the set of environmental controls captures confounding from environmental factors that may be related to both lake levels and transport of PM from other sources. The remaining variation in PM can then reasonably be attributed to lake desiccation, where a location's exposure to playa dust is driven by the distance from the lake and the prevailing wind conditions. We examine the three different types of PM since playa dust is a blend of these particulates (Goodman et al., 2019).

3.2 Second Stage: Health Outcomes

Having established a link between lake desiccation and PM pollution, we next quantify the health impacts due to increased exposure to playa dust using a two-sample two-stage least squares approach. We use the first stage analysis framework to create predictions of playa dust (using $PM_{2.5}$ estimates) at the parental residence over the pregnancy duration.[9] We then regress several health measures on this instrumented exposure, giving us the causal impact of playa dust on infant health.

We predict daily pollution at the county centroids using the first stage frameworks applied to the county level pollution data. We then aggregate the daily predictions over the last trimester (98 days) of pregnancy, using the 15th of the birth month as the birth date.[10] We use an identical aggregation process for the environmental control variables. This process generates the following estimate of playa dust exposure at the parental residence over the last trimester of pregnancy.

$$\text{Playa Dust}_{c\tau} = \frac{1}{98} \sum_{t=\tau-98}^{\tau-1} \hat{\text{PM}}_{2.5ct} \tag{6}$$

We focus on the last trimester since existing work has shown pollution exposure later in pregnancy is the most impactful for birth outcomes (Rich et al., 2015; Hooven et al., 2011).

We estimate the health impact from increased playa dust using the following regres-

[9] We focus on $PM_{2.5}$ to predict playa dust for the health analyses since it is relevant for health outcomes and the PurpleAir data aligns more closely with validated EPA data for $PM_{2.5}$ than for the other particulates (see Figure ??).

[10] The birth data records only birth month and year for each individual.

sion specification.

$$y_{i\tau} = \beta \text{Playa Dust}_{c\tau} + M'_{i\tau}\gamma_1 + E'_{c\tau}\gamma_2 + \alpha_c + \alpha_\tau + \varepsilon_{i\tau} \tag{7}$$

$y_{i\tau}$ denotes a measure of infant health for individual i born in month τ to an individual residing in county c. We measure infant health directly with four commonly used outcomes: term birth weight (birth weight if estimated gestation age is between 37 and 42 weeks), term low birth weight (an indicator for births where gestation age is between 37 and 42 weeks equal to one if birth weight is below 2,500g), preterm birth (an indicator equal to one if the estimated gestation age is less than 37 weeks), and very preterm birth (an indicator equal to one if the estimated gestation age is less than 32 weeks). We differentiate between preterm and term outcomes since term conditional outcomes capture changes in growth restriction seperately from impacts on gestational length.

We condition this relationship on several characteristics of the pregnant individual ($M_{i\tau}$), a set of environmental covariates ($E_{i\tau}$), a linear year trend, and county (α_c) and calendar month (α_τ) fixed effects. The set of individual characteristics consisting of age, race, education, WIC status, private insurance use, and smoking status are included to improve precision of our estimates. The set of environmental controls is identical to those from the first stage, but are averaged over the last trimester. The county fixed effect is based on the pregnant individual's county of residence at the time of birth, while the calendar month fixed effects are based on the infant's birth month. Standard errors are estimated via clustered bootstrapping, where we select a bootstrap sample clustering by county for the first stage and use the same bootstrap sample of counties to estimate the second stage (Björklund and Jäntti, 1997).

4 Results

4.1 First Stage: Air Pollution

We start by documenting a positive relationship between playa area and PM exposure using the simple model (Eq. 4) in combination with pollution monitor level data. The coefficient

Figure 3: Playa Area Effect Gradients

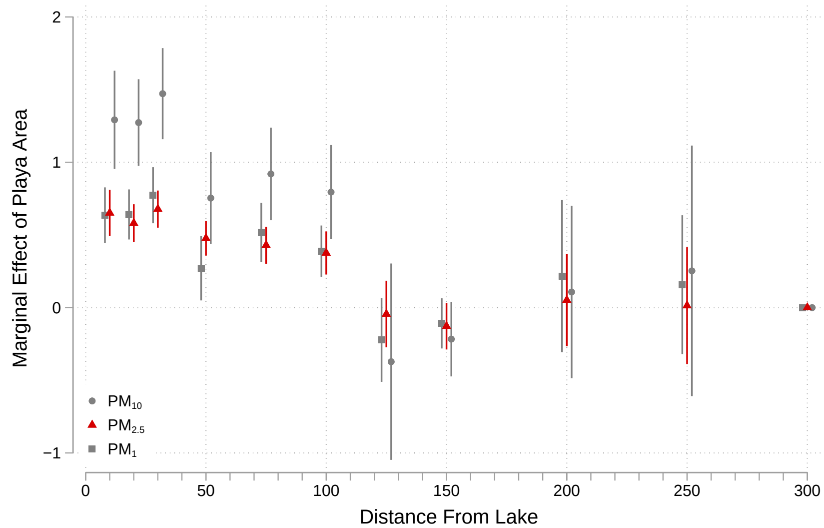

Notes: Figure plots coefficient estimates and 95% confidence intervals for the interaction terms between playa area and distance bins from Eq. 4, run separately for each PM measure. The omitted group is 250-300km. Controls include time and monitor fixed effects and environmental controls. Standard errors are clustered at the monitor level.

gradients over space are shown for each of the three pollutants in Figure 3, with $PM_{2.5}$ highlighted in red. For $PM_{2.5}$, a 100km^2 increase in playa area increases particulate concentrations by about 0.64 $\mu g/\mathrm{m}^3$ within 30 km of the lake. This effect diminishes with distance, as expected, and reaches zero by the 100-150km bin. PM_{10} and PM_1 show similar gradients, though they are relatively noisier. Additionally, PM_{10} shows a relatively large increase due to increased playa area, which aligns with the Great Salt Lake playa dust containing more PM_{10} than $PM_{2.5}$ (Goodman et al., 2019).

To contextualize the scale of these results, moving from the 25th to 75th percentile of playa area over the sample time frame results in a 184km^2 increase in playa, which scales to an average increase of 0.9 $\mu g/\mathrm{m}^3$ in $PM_{2.5}$ within 100km of the lake, or a 14% increase over average $PM_{2.5}$ concentrations.[11] Considering instead the long run change in lake levels and naively assuming a linear relationship between playa area and $PM_{2.5}$, our estimates indicate

[11] The average coefficient within 100km of the lake is calculated as the weighted average across the six relevant coefficients, with weights determined by the distance covered by each bin, and equals 0.49. The 0.9 increase is calculated as 0.49*1.839. The average $PM_{2.5}$ concentration is with respect to the full sample time frame for monitors within 100km of the lake, and equals 6.62.

that $PM_{2.5}$ is $5\mu g/\mathrm{m}^3$ higher than would be the case without lake desiccation. While this is likely an overstatement of the aggregate effect, our marginal effect estimates are actually substantially smaller than similar estimates from the Salton Sea in California, where Jones and Fleck (2020) estimate a $100\mathrm{km}^2$ increase in playa would increase $PM_{2.5}$ concentrations by $2.22\mu g/\mathrm{m}^3$.

We next use the extended model to map the marginal playa effect accounting for variations in playa dust distribution due to wind conditions. The results of this exercise are shown in Figure 4 for each PM measure, separately for winter and summer months. In each map, the center point (0,0) denotes the lake's location, east-west distance is shown on the x-axis, and north-south distance on the y-axis. The marginal effect across space is calculated assuming a wind blowing due east along the x-axis of average speed.

For all predictions, playa area significantly increases PM concentrations close to the lake, with diminishing effects further away. In line with the simplified model, the largest effects appear to occur within around 30km of the lake. In contrast to the simplified model, the estimates of effect magnitude from the extended model are significantly higher and more variable, with hot spots of exposure seeing $PM_{2.5}$ increase by over $2\mu g/\mathrm{m}^3$. The figures also document surprising variation by seasonality. Across both seasons, a general plume of increased PM covers the downwind areas. However, in summer months, the largest effects are in areas immediately downwind of the lake, while in winter months the areas immediately upwind of the lake are the most affected. Further data is needed to understand exactly why this pattern occurs, but it may reflect microclimates occurring near the lake borders.

Overall, Figures 3 and 4 document significant spatial and temporal variation in the impact on PM due to changes in playa area. This finding is important in its own right, in that we show lake desiccation has meaningful impacts on local air quality. Additionally, the spatial variation in effect from both models and the statistical precision of the simple model estimates suggest that econometric models are sufficient to capture air quality changes, so that more computationally intensive models (like particle transport models) are not necessary to capture average local pollution changes. Lastly, these results provide a foundation for identifying exogenous variation in playa dust since they show that, with sufficient temporal and spatial variation, exogenous changes in playa area and wind conditions drive changes in

Figure 4: Playa Area Effect Contour Plots

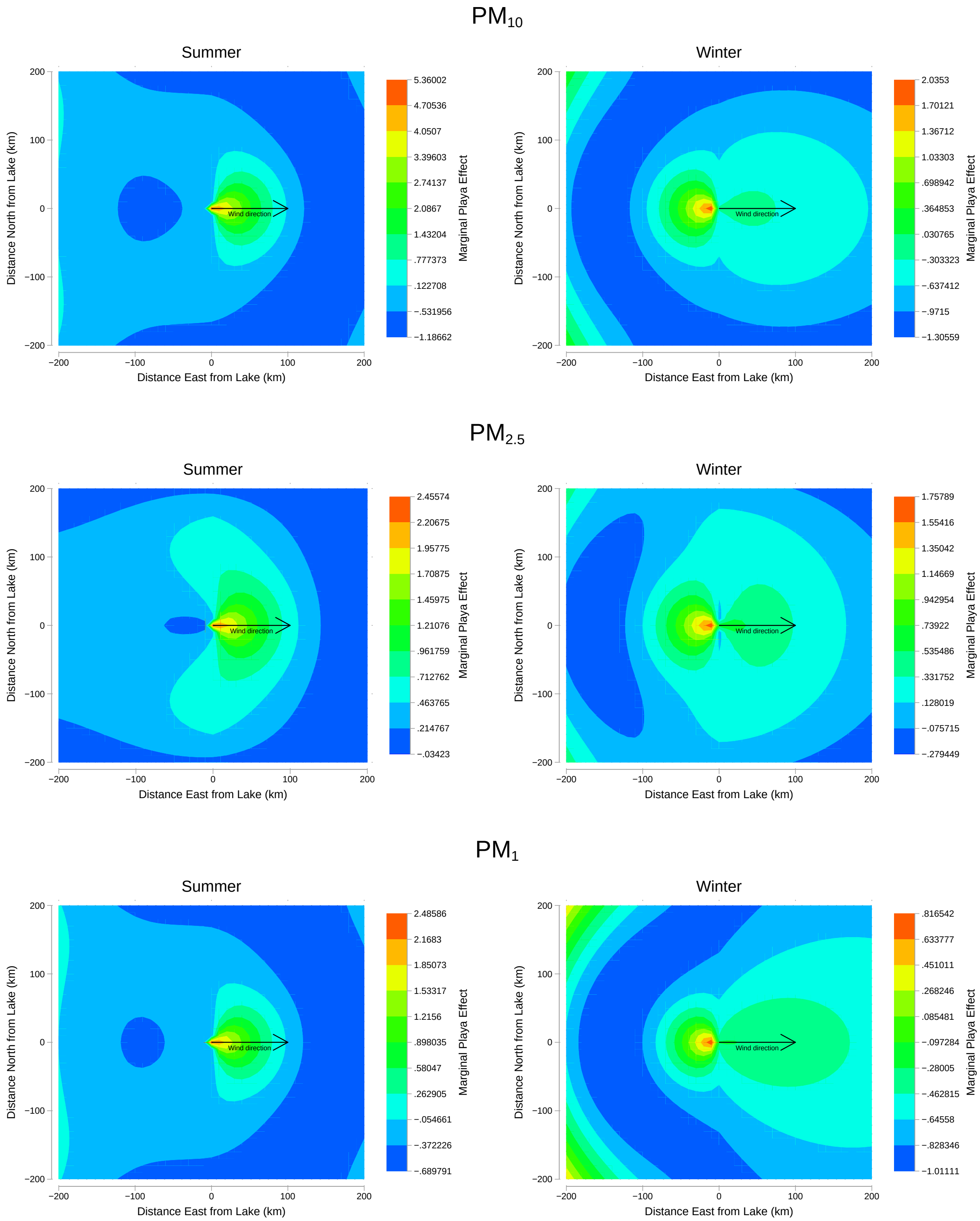

Notes: Figure maps the estimated marginal effect of a 100km^2 increase in playa area over space predicted by Eq. 5, separately for each PM measure and season. The point (0,0) denotes the lake's location, east-west distance is shown on the x-axis, and north-south distance on the y-axis. Marginal effects assume a wind of average speed blowing along the x-axis towards the east, denoted by the black arrow. Controls include calendar-month and monitor fixed effects, a linear year trend, and environmental controls.

$PM_{2.5}$ exposure.

4.2 First Stage to Second Stage: Testing Assumptions

To quantify the health effects attributable to lake desiccation, we use identical frameworks as Equations 4 and 5 to predict exogenous changes in playa dust at the county centroid over the last three months of pregnancy. For the subsequent health analyses to return the causal effect of interest, we need the predicted playa dust to be conditionally exogenous (exclusion) and reflective of the true pollution (relevance). The exclusion restriction holds given the necessary assumptions underlying the difference-in-difference analyses are true. Specifically, the first stage analyses assume $PM_{2.5}$ patterns would have conditionally trended similarly over time and space in absence of changes in lake levels. For the relevance condition, the monitor level analyses serve as a proof of concept for predicting playa dust concentrations. However, it is possible that with the necessary aggregation over space and time to align with the birth data the instruments for playa dust lose power and violate the relevance condition.

We verify the exclusion restriction by documenting that predicted playa dust is conditionally uncorrelated with characteristics of the pregnant individual that are in turn correlated with infant health. For this analysis, we regress covariates from the birth data on the playa dust predictions, following Equation 7 but omitting individual controls $M_{i\tau}$. The results are shown in Table 2. Across all demographic covariates in columns 1-7, both models show no meaningful relationship with playa dust, validating that the instrumental variables are not influencing infant health through correlations with parental covariates. Columns 8 and 9 do show statistically significant relationships between WIC and private insurance use, however further examination of the data suggests this relationship arises from a trend break in WIC and private insurance use in March 2022, when lake levels were relatively low (see Figure A2 in the Appendix). Removing the data after this period mostly eliminates the observed relationships, with respect to both statistical significance and magnitude.

We check instrument strength for the second stage by repeating our first stage analyses at different levels of aggregation and reporting the F-statistics from tests of joint significance on the interaction terms. The results of this process are shown in Table 3. Column 1 shows the F-statistics for the daily monitor level analyses shown above, where for both models

Table 2: Playa Dust and Parental Covariates

	(1) White	(2) Black	(3) Hispanic	(4) Bachelors	(5) Married	(6) Age	(7) Smoked	(8) WIC Use	(9) Private Insurance
Panel A: Simple Model									
Playa Dust	-0.0013	0.0001	0.0025	-0.0027	-0.0029	-0.0107	0.0006	0.0128***	-0.0206*
	(0.0018)	(0.0008)	(0.0025)	(0.0064)	(0.0041)	(0.0427)	(0.0011)	(0.0049)	(0.0111)
Panel B: Extended Model									
Playa Dust	0.0001	0.0000	0.0025	0.0014	-0.0030	-0.0235	0.0009	0.0126***	-0.0221**
	(0.0025)	(0.0007)	(0.0025)	(0.0060)	(0.0028)	(0.0329)	(0.0011)	(0.0038)	(0.0097)
Sample Mean	0.9064	0.0162	0.1830	0.3767	0.8108	28.7437	0.0224	0.1656	0.6484
Observations	243,626	243,626	238,978	237,273	243,526	243,626	242,736	237,322	243,626

Notes: Table presents coefficient estimates from regressions of parental covariates on predicted playa dust following Eq. 7. All results control for environmental controls, a linear year trend, and calendar-month and county fixed effects. Each column is an outcome variable. Panel A uses playa dust predicted by Eq. 4 and Panel B uses playa dust predicted by Eq. 5. Bootstrapped standard errors are clustered at the county level. $***p < 0.01, **p < 0.05, *p < 0.1$.

the F-statistic is well above the rule-of-thumb cutoff for weak instruments of 10. Column 2 reports the F-statistics after rerunning the analyses at the centroid level, using the IDW air pollution measure (Eq. 1) as the left hand side variable. For both models, the F-statistics are again above 10. Columns 3 and 4 next aggregate to align with the timing of the birth sample, measuring pollution and all right hand side environmental and weather variables with the average over the three months (98 days) before the 15th of each month. For the monitor sample (Column 3), the instruments appear to still be sufficiently powered, though relatively weaker than the daily sample. For the centroid sample (Column 4), the F-stat for the simple model is indicative of a potentially weak instrument. The extended model in contrast shows a large F-stat, though this may be due to overfitting the data due to the loss of variation in wind conditions arising from temporal smoothing. Overall, the results of this exercise advise some caution, since after aggregating to the county - trimester level there may be weak instrument bias.

4.3 Second Stage: Health Outcomes

The main results show that lake desiccation is associated with adverse health outcomes. Using the simple model to predict $PM_{2.5}$, we find a $1\mu g/m^3$ increase of playa dust increases

Table 3: Aggregated Sample F-Statistics

	(1) Daily Monitor	(2) Daily Centroid	(3) 3-month Monitor	(4) 3-month Centroid
Simple Model	24.07	14.66	17.78	4.48
Extended Model	47.70	293.39	11.25	222.32
Point	Monitor	County centroid	Monitor	County centroid
Time	Day	Day	3-months	3-months
Observations	564,749	58,036	7,854	1,639

Notes: Table reports F-statistics from tests of joint significance on the interaction terms from the first stage models, each run sperately. The simple model denotes Eq. 4 and extended model denotes Eq. 5. Each column reflects a different level of sample aggregation. Column 1 is at the pollution monitor-day level. Columns 2 and 4 aggregate to county level. Columns 3 and 4 aggregate to the average over the three months preceeding the 15th of each month. Standard errors are clustered at the respective point (monitor or county centroid) level.

the probability of preterm birth by 0.09 percentage points (1% over average rates) and of very preterm birth by 0.07 percentage points (8%). Conditional on making it to term, we find birth weight decreases by 3.78g with the probability of being classified as low birth weight increasing by 0.1 percentage points (4%). Additionally, we find the number of live births each month in a county decreases by about 4% with increased playa dust, which if we assume playa dust is exogenous to conception rates would suggest increased rates of unobserved pregnancy loss. We find similar effects for all outcomes when using $PM_{2.5}$ predictions from the extended model as well.

Our estimated health effects are slightly larger than the average health impacts of $PM_{2.5}$, as estimated in a meta-analysis by Stieb et al. (2012). With respect to preterm birth rates, the meta-analysis estimates the average odds ratio from a $10\mu g/\mathrm{m}^3$ increase in $PM_{2.5}$ to be 1.05, with a 95% confidence interval bounded by 0.98 and 1.13. Scaling our estimate, our results indicate a 1.11 odds ratio from an equivalent increase in playa dust, which is larger but still within the confidence interval of the average estimate. Similarly for birth weight, the meta-analysis reports an average 23.4g decrease in birth weight per $10\mu g/\mathrm{m}^3$ increase in $PM_{2.5}$, with a 95% confidence interval bounded by 1.4 and 45.5.[12] Our estimate which scales

[12]The meta-analysis reports the effect on birth weight based on $PM_{2.5}$ exposure over the pregnancy duration, rather than only the last trimester of pregnancy. If only pollution in the last trimester impacts birth weight (Rich et al., 2015), an argument can be made that averaging pollution over the pregnancy duration rather than the last trimester may make the meta-analysis lower than the relevant estimate if based on the last trimester alone.

Table 4: Health

	(1)	(2)	(3)	(4)	(5)
	Preterm	Very Preterm	Term Birth Weight	Term Low Birth Weight	Live Births
Panel A: Simple Model					
Playa Dust	0.0009	0.0007	-3.7803	0.0010	-7.7017
	(0.0020)	(0.0007)	(2.7731)	(0.0010)	(14.6877)
Panel B: Extended Model					
Playa Dust	0.0018	0.0005	-3.3840	0.0004	-3.6209
	(0.0022)	(0.0004)	(2.9713)	(0.0013)	(6.4804)
Sample Mean	0.0876	0.0087	3356.8266	0.0231	186.5436
Observations	230,227	230,227	210,070	210,070	1,306

Notes: Table presents coefficient estimates from regressions of infant health outcomes on predicted playa dust following Eq. 7. All results control for environmental controls, parental controls, a linear year trend, and month and county fixed effects. Each column is an outcome variable. Panel A uses playa dust predicted by Eq. 4 and Panel B uses playa dust predicted by Eq. 5. Bootstrapped standard errors are clustered at the county level. $***p < 0.01, **p < 0.05, *p < 0.1$

to a 35g reduction is again larger but within the confidence interval. The larger estimated health effects from playa dust rather than $PM_{2.5}$ could potentially reflect additional adverse effects from the playa composition. In addition to PM, Great Salt Lake playa contains arsenic and mercury (Jung et al., 2024), which if transported with the measurable $PM_{2.5}$ could lead to more severe health effects. Further research is needed to confirm this hypothesis.

We use our analyses to estimate the financial cost due to health expenditures, and find significant losses from desiccation. We focus exclusively on the direct medical expenses due to preterm births which are estimated to be $22,690 per preterm birth (gestation age 32-36 weeks) (Behrman and Butler, 2007). This restriction means our estimated financial cost will be a significant understatement, since it ignores factors like later life costs ($3,163) and additional costs from very preterm babies (up to $176,846). To extrapolate to the full range of lake elevations, we repeat our main analysis on an expanded sample, predicting Playa Dust$_{c\tau}$ for births occurring between 2009 and 2022.[13] Additionally, we include the square of Playa Dust$_{c\tau}$ to allow for non-linear health changes. The results from this are shown in Table A1. We then translate the effect on preterm births into a marginal cost of playa area which

[13] We assume the first stage relationship between playa area and dust holds across the alternative playa areas in the longer sample.

is plotted in Figure 5. We see the marginal cost can be significant, peaking at $1,877,396 (about 83 preterm babies). In line with existing work, the marginal cost diminishes with more exposed playa, reflecting that additional PM is less impactful when PM is already high (Weichenthal et al., 2022; Vodonos, Awad, and Schwartz, 2018).

We then compare the estimated marginal health costs with an approximation of the marginal cost to increase water in the lake, arguably the most straight forward solution to mitigating desiccation. We assume that the only cost of adding water to the lake is the monetary cost of purchasing the water, which we estimate using data on one year water leases in the Western US (Brewer et al., 2008).[14][15] We plot the marginal cost generated by the 25th, 75th, and 100th percentile of these prices in Figure 5 for comparison to the marginal health costs. For additional context, the Office of the Legislative Auditor General released a report in 2023 that estimated an "annual maintenance [cost] of $15 million" for dust mitigation on the Great Salt Lake (Utah OLAG, 2023). Given current exposed playa area (1,059km^2), this translates into a water price of $57.32.

We see that relative to the marginal health cost, the marginal water cost is insignificant for the majority of the price distribution and only for very high water costs are the two comparable. With respect to mitigation efforts, this means that given current lake levels (vertical dashed line) and the modeling assumptions, it is optimal to purchase water and refill the lake so that there is zero exposed playa area for the majority of the water price distribution. For the highest water price, it is still optimal to refill the lake (the total benefit exceeds total cost, shown visually by the shaded areas), though doing so would require paying for some water in excess of its marginal benefit with respect to health in order to move along the curve towards more beneficial mitigation levels. This raises an interesting dynamic then for policy makers: When lake levels are extremely low the marginal benefit of covering playa is also very low. Therefore, as lake levels decline there becomes a point where it is inefficient to add water to the lake since a significant share of playa must be covered before

[14]It is a potentially strong assumption that there are no other costs associated with refilling the lake, however given that the lake is a terminal lake such that all water in the hydrologic basin eventually flows to it, an argument can be made that the need for infrastructure is limited.

[15]We focus on the subset of water trades which occur between agricultural water rights holders and environment based water users. Water prices are reported in inflation adjusted price per acre foot, in 2025 dollars.

Figure 5: Playa Area Mitigation Cost-Benefit

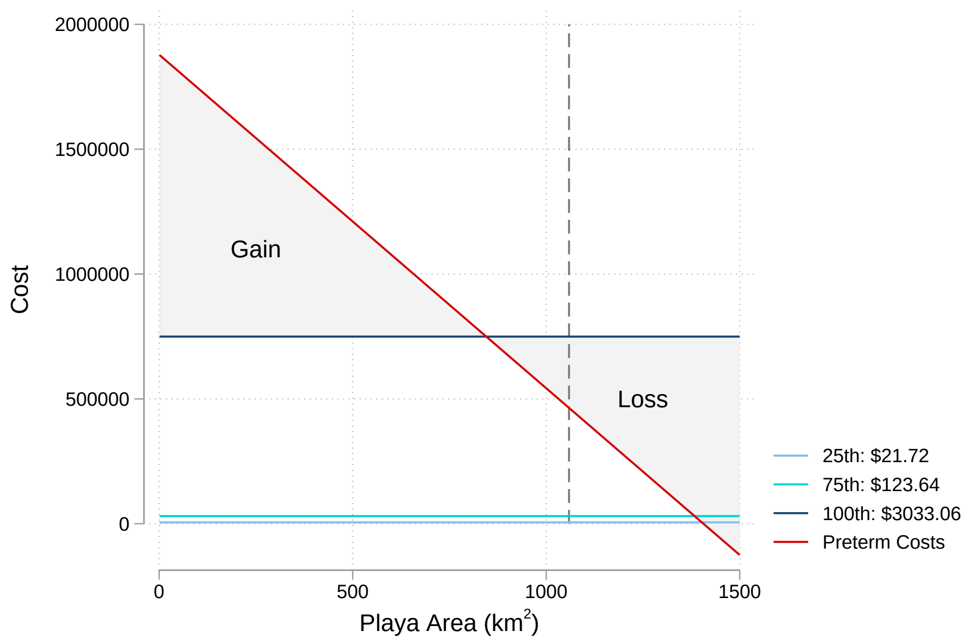

Notes: Figure plots marginal costs of playa exposure and mitigation efforts. Preterm costs denotes marginal cost of exposed playa area due to direct medical expenditures due to preterm births. Marginal costs estimated using coefficient estimates from Table A1. Mitigation effort marginal costs are based on the marginal cost of water to cover exposed playa area, with costs derived from three different percentiles of the distribution of water trade prices: 25th, 75th, 100th. Water prices are in 2025 dollars per acre-foot of water. Lake levels as of January 2025 are denoted by the vertical dashed line. The gray shaded areas between the preterm cost curve and the maximum mitigation marginal cost curve denote where marginal mitigation costs are less then the marginal preterm costs (gain) or greater than (loss).

any meaningful health gains are made. In contrast, if the lake is prevented from declining too much then it will always be beneficial to pay the water cost to cover the smaller playa area since it has large marginal benefits.

4.4 Robustness Checks

We examine the extent that weak instruments are biasing our estimated health effects, and find that while there likely is bias, it is attenuating our effects towards the null. To examine the role of weak instrument bias, we compare our main health results to an OLS specification which is identical to Eq. 7, except which uses observed $PM_{2.5}$ as the variable of interest (Table A2). If there is weak instrument bias, our main effects will be biased towards the OLS estimates. For the simple model, we find that the instrumented effects are consistently much larger than the OLS estimates, suggesting the bias is not extreme. Furthermore, if there is weak instrument bias it will be more severe with more instruments. For the instrument heavy extended model, the estimates are generally attenuated toward the OLS estimates relative to the simple model. In combination, the results from this exercise show there is likely some degree of weak instrument bias, though it is driving attenuation of our effect estimates.

We also test the robustness of our health results to several alternative specifications. First, we re-estimate our main specification weighting the first stage regressions by the number of births observed in each county-month. The estimated effects, shown in Table A3, and directionally similar but smaller in magnitude than our main effects. Second, we re-estimate our main specification incorporating month-of-sample fixed effects in the second stage, Table A4. The resulting coefficients are less precisely estimated and are sometimes differently signed, though the extended model is generally more similar to the main specification, potentially reflective of more spatial variation in Playa Dust$_{c\tau}$ for identification. Third, we repeat the main analysis on the extended sample of births from 2009-2022, with Table A1 showing similar effect estimates for preterm and very preterm but not the other three outcomes. Lastly, in Table A5 we use a reduced form specification to estimate the health effects, plugging the simple model instruments directly into the second stage.[16]. With respect

[16]We focus exclusively on the simple model since the extended model coefficients are difficult to interpret

to the omitted distance bin (100-300km), the results are inconsistent with our main effects. However, comparing the within 10km group to the other within 100km groups does generally align with our main results, potentially reflective of the changes in $PM_{2.5}$ being concentrated in close proximity to the lake. Overall, our results are not especially robust to alternative specifications, though finer grained geocoding of the birth data is likely to remediate some of these issues.

5 Conclusion

The findings of this paper establish that desiccation of the Great Salt Lake increases local air pollution leading to subsequent associations with adverse health impacts. By exploiting exogenous exposure to playa dust driven by wind and lake conditions, we find a 100km^2 increase in playa area increases $PM_{2.5}$ by $0.49\mu g/m^3$ within 100km of the lake. This finding indicates lake desiccation has large impacts on air quality both with respect to magnitude and spatial extent. The worsened air quality translates into associations with adverse health outcomes, with the probability of preterm birth increasing by 1% and birth weight decreasing by 3.78g per 100km^2 of playa area.

Our analysis is subject to some data limitations which may lead to our estimates to be biased or suffer from limited external validity. In particular, we use birth record data that is geocoded at the county level and contains only the birth month and year. This requires us to aggregate our data significantly and leads to weakening of our identification strategy, potentially leading towards downward bias of our health effect estimates. Additionally, we use the parental residence at time of delivery, which may not accurately reflect exposure if the pregnant individual moved or spent a significant amount of time outside of their residence (ie. at work) during pregnancy. Lastly, the time frame of available PurpleAir data is relatively short compared to the timeline of desiccation for the Great Salt Lake. This results in us potentially missing important nonlinearities in the first stage analysis that would arise at low playa area levels.

Overall the findings from this paper emphasize the importance of accounting for health externalities associated with lake desiccation when considering water resource management.

Our simple back-of-the envelope exercise estimates annual total costs from desiccation reaching $1.2 billion at current lake levels due just to preterm birth incidence. This is in contrast to our back of the envelope estimated mitigation costs ranging between $5.7 million and $794 million, as well as estimates from the Utah Legislature of an upfront cost of lake mitigation of $1.5 billion and annual maintenance cost of $15 million (Utah OLAG, 2023). The large adverse health consequences due to lake desiccation underscore the an often overlooked ecologic service provided by water systems: dust mitigation.

References

Abman, Ryan, Eric C. Edwards, and Danae Hernandez-Cortes (2024). "Water, dust, and environmental justice: The case of agricultural water diversions". In: *American Journal of Agricultural Economics*, pp. 1–18.

Attah, Reuben et al. (2024). "Assessing the Oxidative Potential of Dust from Great Salt Lake". In: *Atmospheric Environment* 336, pp. 1–11.

Barkjohn, Karoline, Andrea Clements, and Amara Holder (2022). "ORD Updates: AirNow Fire and Smoke Map". In: US Environmental Protection Agency.

Baskin, Robert L. (2005). "Calculation of Area and Volume for the Sorth Part of Great Salt Lake, Utah". In: pp. 1–6.

— (2006). "Calculation of Area and Volume for the North Part of Great Salt Lake, Utah". In: pp. 1–6.

Behrman, R.E. and A.S. Butler (2007). *Preterm Birth: Causes, Consequences, and Prevention. Institute of Medicine (US) Committee on Understanding Premature Birth and Assuring Healthy Outcomes*. National Academies Press.

Björklund, Anders and Markus Jäntti (1997). "Intergenerational Income Mobility in Sweden Compared to the United States". In: *The American Economic Review* 87.5, pp. 1009–1018.

Brewer, Jedidiah et al. (2008). "Water Markets in the West: Prices, Trading and Contractual Forms". In: *Economic Inquiry* 46.2, pp. 91–112.

Currie, Janet and Reed Walker (2011). “Traffic Congestion and Infant Health: Evidence from E-ZPass”. In: *American Economic Journal: Applied Economics* 3.1, pp. 65–90.

Farzan, Shohreh F. et al. (2019). “Assessment of Respiratory Health Symptoms and Asthma in Children near a Drying Saline Lake”. In: *International Journal of Environmental Research and Public Health* 16.3828, pp. 1–15.

Gomez, Stephen R. et al. (1992). “Respiratory Health Effects of Alkali Dust in Residents Near Desiccated Old Wives Lake”. In: *Archives of Environmental Health* 47.5, pp. 364–369.

Goodman, Michael M. et al. (2019). “Trace element chemistry of atmospheric deposition along the Wasatch Front (Utah, USA) reflects regional playa dust and local urban aerosols”. In: *Chemical Geology* 530, pp. 1–11.

Hill, Elaine et al. (2024). “Roadway construction as a natural experiment to examine air pollution impacts on infant health”. In: *Environmental Research* 252.2, pp. 1–9.

Hooven, Edith H. van den et al. (2011). “Air Pollution Exposure During Pregnancy, Ultrasound Measures of Fetal Growth, and Adverse Birth Outcomes: A Prospective Cohort Study”. In: *Environmental Health Perspectives* 120.1, pp. 150–156.

Jones, Benjamin A. and John Fleck (2020). “Shrinking lakes, air pollution, and human health: Evidence from California’s Salton Sea”. In: *Science of the Total Environment* 712, pp. 1–13.

Jung, Julie et al. (2024). “Toxic elements in benthic lacustrine sediments of Utah’s Great Salt Lake following a historic low in elevation”. In: *Frontiers in Soil Science* 4.

Kim, Seung Min and Kenneth T. Gillingham (2025). “Air Pollution and Solar Energy: Evidence from Wildfires”. In: *Journal of the Association of Environmental and Resource Economists* 12.2, pp. 493–526.

King, James et al. (2011). “Dust emission variability at the Salton Sea, California, USA”. In: *Aeolian Research* 3.1, pp. 67–79.

Legislative Auditor General, Office of the (2023). *High-Risk List: Identifying and Mitigating Critical Vulnerabilities in Utah.* 2023-10, pp. 1–128.

Perry, Kevin D., Erik T. Crosman, and Sebastian W. Hoch (2019). *Results of the Great Salt Lake Dust Plume Study*, pp. 1–319.

Rich, David Q. et al. (2015). “Differences in Birth Weight Associated with the 2008 Beijing Olympics Air Pollution Reduction: Results from a Natural Experiment”. In: *Environmental Health Perspectives* 123.9, pp. 880–887.

Schlenker, Wolfram and W. Reed Walker (2016). “Airports, Air Pollution, and Contemporaneous Health”. In: *The Review of Economic Studies* 83.2, pp. 768–809.

Stieb, David M. et al. (2012). “Ambient air pollution, birth weight and preterm birth: A systematic review and meta-analysis”. In: *Environmental Research* 117, pp. 100–111.

US Environmental Protection Agency (2017). *Owens Valley Particulate Matter Plan Q & A*. URL: https://19january2017snapshot.epa.gov/www3/region9/air/owens/qa.html.

— (2024). *National Ambient Air Quality Standards (NAAQS) for PM*. URL: https://www.epa.gov/pm-pollution/national-ambient-air-quality-standards-naaqs-pm.

Vodonos, Alina, Yara Abu Awad, and Joel Schwartz (2018). “The concentration-response between long-term PM2.5 exposure and mortality; A meta-regression approach”. In: *Environmental Research* 166, pp. 677–689.

Weichenthal, Scott et al. (2022). “How low can you go? Air pollution affects mortality at very low levels”. In: *Science Advances* 8.39.

Wurtsbaugh, Wayne A. et al. (2017). “Decline of the world’s saline lakes”. In: *Nature Geoscience* 10, pp. 816–821.

6 Appendix

A Supplemental Figures

B Supplemental Tables

Figure A1: EPA Pollution vs IDW PurpleAir Pollution

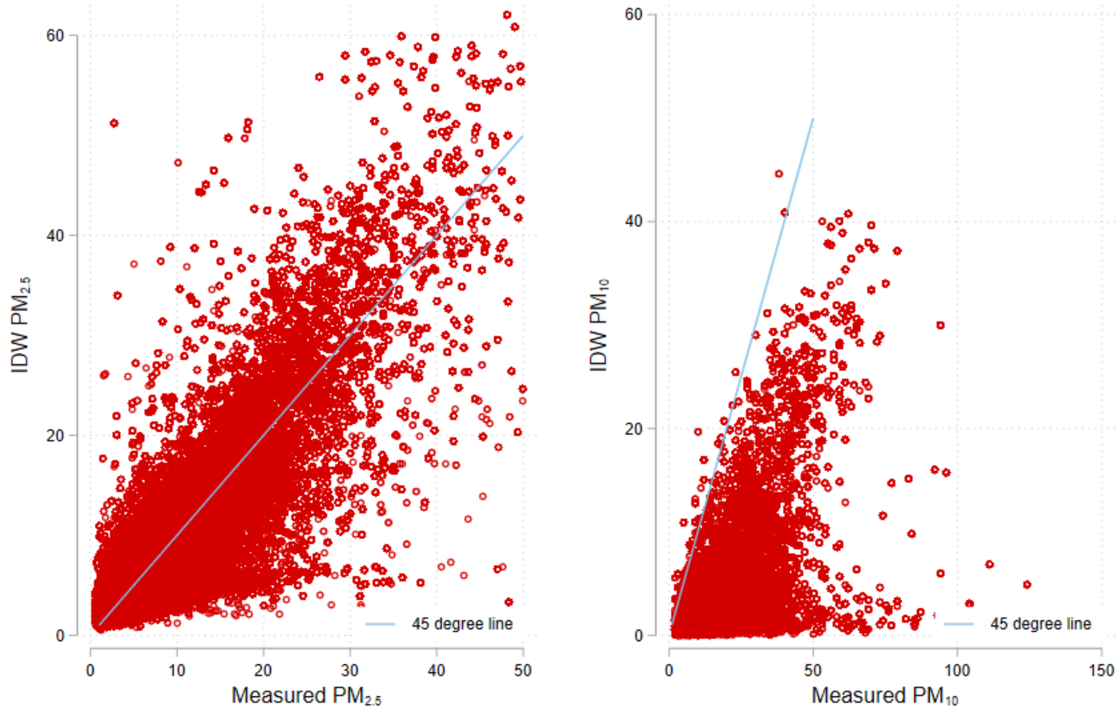

Notes: Left panel of figure plots measured $PM_{2.5}$ from EPA operated monitors against predicted $PM_{2.5}$ concentrations based on IDW averages of PurpleAir monitors following Eq. 1. Right panel of figure plots the same for PM_{10}. PM levels are measured in $\mu g/\mathrm{m}^3$.

Figure A2: Trends in WIC and Private Insurance Use

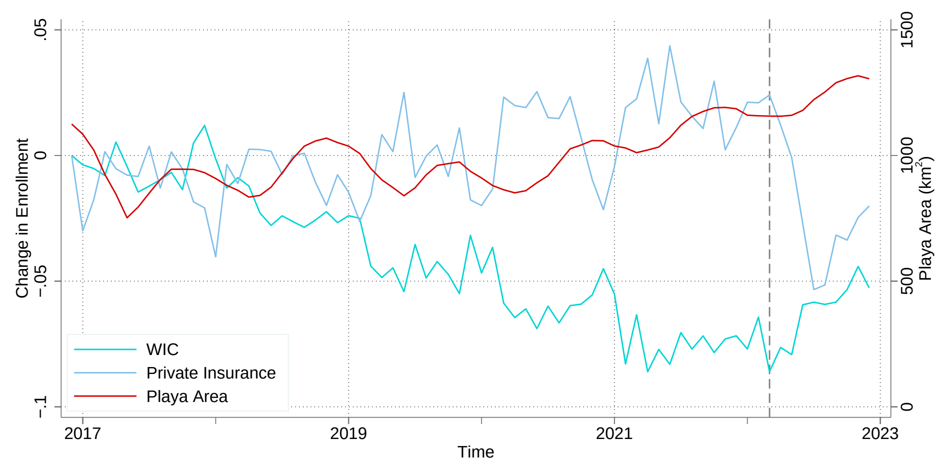

Notes: Figure plots the change over time in the share of individuals reporting WIC and private insurance use in the birth sample on the left y-axis. Exposed playa area over time is shown on the right y-axis.

Table A1: Health Effects on Full Birth Sample

	Preterm		Very Preterm		Term Birth Weight		Term Low Birth Weight		Live Births	
Panel A: Simple Model										
Playa Dust	0.0017	0.0036***	0.0002	0.0004	0.6812	1.1529	-0.0001	0.0008*	3.1010	8.5796
	(0.0011)	(0.0025)	(0.0003)	(0.0002)	(0.8192)	(0.0005)	(0.0005)	(0.0000)	(6.7847)	(2.3631)
Playa Dust^2		-0.0002		-0.0000		-0.0421		-0.0001		-0.6639
		(0.0025)		(0.0002)		(0.0005)		(0.0000)		(2.3631)
Panel B: Extended Model										
Playa Dust	0.0028**	0.0027**	0.0006*	0.0014***	0.5875	3.6888**	0.0000	0.0020***	2.6394	15.4547***
	(0.0013)	(0.2463)	(0.0003)	(0.0006)	(1.4849)	(0.0001)	(0.0006)	(10.4288)	(4.1835)	(0.7478)
Sample Mean	0.0873	0.0873	0.0088	0.0088	3363.8913	3363.8913	0.0220	0.0220	156.2172	156.2172
Observations	553,951	553,951	553,951	553,951	505,614	505,614	505,614	505,614	8,744	8,744

Notes: Table presents coefficient estimates from regressions of infant health outcomes on predicted playa dust using the sample of births from 2009 through 2022. All results control for environmental controls, parental controls, a linear year trend, and month and county fixed effects. Each column is an outcome variable. Panel A uses playa dust predicted by Eq. 4 and Panel B uses playa dust predicted by Eq. 5. Bootstrapped standard errors are clustered at the county level. $***p < 0.01, **p < 0.05, *p < 0.1$

Table A2: Health Effects OLS

	(1) Preterm	(2) Very Preterm	(3) Term Birth Weight	(4) Term Low Birth Weight	(5) Live Births
$PM_{2.5}$	0.0002	0.0001	0.2080	0.0000	-1.7207
	(0.0003)	(0.0001)	(0.6711)	(0.0001)	(1.0617)
Sample Mean	0.088	0.009	3,355.979	0.023	204.120
Observations	212,578	212,578	193,954	193,954	1,103

Notes: Table presents coefficient estimates from regressions of infant health outcomes on observed $PM_{2.5}$ levels. All results control for environmental controls, parental controls, a linear year trend, and month and county fixed effects. Each column is an outcome variable. Standard errors are clustered at the county level. $***p < 0.01, **p < 0.05, *p < 0.1$

Table A3: Health Effects With Weights

	(1) Preterm	(2) Very Preterm	(3) Term Birth Weight	(4) Term Low Birth Weight	(5) Live Births
Panel A: Simple Model					
Playa Dust	0.0004	0.0003	-1.7173	0.0005	-2.3434
	(0.0009)	(0.0003)	(1.4124)	(0.0005)	(9.4110)
First Stage F-stat	3,070.69	3,070.69	3,070.69	3,070.69	3,070.69
Panel B: Extended Model					
Playa Dust	0.0010	0.0003	-0.6966	-0.0003	-2.8404
	(0.0022)	(0.0005)	(2.6302)	(0.0012)	(4.7575)
First Stage F-stat	2,657.63	2,657.63	2,657.63	2,657.63	2,657.63
Sample Mean	0.0876	0.0088	3356.8293	0.0231	194.1938
Observations	230,122	230,122	209,971	209,971	1,254

Notes: Table presents coefficient estimates from regressions of infant health outcomes on predicted playa dust, weighting observations in the first stage analysis by the number of births that occur in a county-month. All results control for environmental controls, parental controls, a linear year trend, and month and county fixed effects. Each column is an outcome variable. Panel A uses playa dust predicted by Eq. 4 and Panel B uses playa dust predicted by Eq. 5. Bootstrapped standard errors are clustered at the county level. $***p < 0.01, **p < 0.05, *p < 0.1$

Table A4: Health Effects With FE

	(1) Preterm	(2) Very Preterm	(3) Term Birth Weight	(4) Term Low Birth Weight	(5) Live Births
Panel A: Simple Model					
Playa Dust	-0.0179*	0.0004	13.2500	-0.0029	-15.8174
	(0.0105)	(0.0032)	(10.1114)	(0.0046)	(32.4137)
Panel B: Extended Model					
Playa Dust	0.0020	0.0006	-1.0992	-0.0034	-0.7190
	(0.0047)	(0.0016)	(7.6992)	(0.0026)	(10.5074)
Sample Mean	0.0876	0.0087	3356.8266	0.0231	186.5436
Observations	230,227	230,227	210,070	210,070	1,306

Notes: Table presents coefficient estimates from regressions of infant health outcomes on predicted playa dust including month-of-sample fixed effects in the second stage analysis. All results control for environmental controls, parental controls, and county fixed effects. Each column is an outcome variable. Panel A uses playa dust predicted by Eq. 4 and Panel B uses playa dust predicted by Eq. 5. Bootstrapped standard errors are clustered at the county level. $***p < 0.01, **p < 0.05, *p < 0.1$

Table A5: Health Effects on Reduced Form

	(1) Preterm	(2) Very Preterm	(3) Term Birth Weight	(4) Term Low Birth Weight	(5) Live Births
Panel A: Without Time FE					
< 10km	-0.0002	0.0005	2.1141	-0.0019	-14.7673***
	(0.0026)	(0.0011)	(1.8322)	(0.0012)	(1.2201)
10-25km	-0.0011	0.0006	4.5684*	-0.0010	-0.4356
	(0.0027)	(0.0012)	(2.5494)	(0.0012)	(2.8497)
25-50km	-0.0035	0.0001	4.5506**	-0.0011	-12.9961
	(0.0026)	(0.0011)	(1.8497)	(0.0013)	(11.7142)
50-100km	-0.0017	0.0003	4.0962*	-0.0013	-0.4210
	(0.0027)	(0.0011)	(2.0629)	(0.0012)	(0.7852)
Panel B: With Time FE					
< 10km	-0.0011	0.0005	2.3009	-0.0018	-14.4084***
	(0.0028)	(0.0011)	(1.9933)	(0.0012)	(1.4660)
10-25km	-0.0022	0.0005	3.9509	-0.0008	0.1746
	(0.0028)	(0.0011)	(2.5778)	(0.0012)	(2.8528)
25-50km	-0.0043	0.0002	4.1660*	-0.0008	-12.5032
	(0.0030)	(0.0011)	(2.2269)	(0.0012)	(11.8057)
50-100km	-0.0029	0.0003	3.8900*	-0.0012	0.1318
	(0.0028)	(0.0011)	(2.1691)	(0.0012)	(0.9585)
Sample Mean	0.0876	0.0087	3356.8266	0.0231	186.5436
Observations	230,227	230,227	210,070	210,070	1,306

Notes: Table presents coefficient estimates from regressions of infant health outcomes on distance from the lake, playa area, and their interaction. All results control for environmental controls, parental controls, a linear year trend, and month and county fixed effects. Each column is an outcome variable. Standard errors are clustered at the county level. $***p < 0.01, **p < 0.05, *p < 0.1$